Original article

Alterations in chemokine receptor CCR5 activity influence tumor cell biology in human cholangiocarcinoma cell lines

Jiaqi Yang [a], David Sontag [b], Yuewen Gong [b], Gerald Y. Minuk [a,b,*]

[a] Section of Hepatology, Department of Internal Medicine, Rudy Faculty of Medicine, University of Manitoba, Winnipeg, Manitoba, Canada
[b] College of Pharmacy, University of Manitoba, Winnipeg, Manitoba, Canada

ARTICLE INFO

ABSTRACT

Introduction and objectives: Intrahepatic (I-CCA) and extrahepatic (E-CCA) cholangiocarcinoma (CCA) have different growth patterns and risks for tumor metastasis. Inhibition and/or activation of the chemokine receptor CCR subclasses have been reported to alter tumor cell biology in non-CCA cancers. In this study we documented CCR expression profiles in representative human I-CCA and E-CCA cell lines and the in vitro effects of CCR antagonists and agonists on tumor cell biology.

Materials and methods: CCR expression profiles were documented by real-time reverse transcription polymerase chain reaction; cell proliferation by WST-1; spheroid formation by sphere dimensions in anchorage-free medium; cell migration by wound healing and invasion by Transwell invasion chambers.

Results: All 10 CCR motifs (CCR1-10) were expressed in the I-CCA, HuCCT1 cell line and six (CCR4, 5, 6, 8, 9 and 10) in the E-CCA, KMBC cell line. In HuCCT1 cells, CCR5 expression was most abundant whereas in KMBC cells, CCR6 followed by CCR5 were most abundant. The CCR5 antagonist Maraviroc significantly inhibited cell proliferation, migration and invasion in HuCCT1 cells, and spheroid formation and invasion in KMBC cells. The CCR5 agonist RANTES had no effect on HuCCT1 cells but increased cell proliferation, migration and invasion of KMBC cells.

Conclusion: These results suggest that CCR expression profiles differ in I-CCA and E-CCA. They also indicate that CCR5 antagonists and agonists have cell-specific effects but in general, CCR5 inactivation inhibits CCA tumor cell aggressiveness. Additional research is required to determine whether CCR5 inactivation is of value in the treatment of CCA in humans.

1. Introduction

Cholangiocarcinoma (CCA) is the most common primary malignancy of the biliary tract. Traditionally, CCAs are divided into intrahepatic and extrahepatic (including hilar and distal duct) tumors (I-CCA and E-CCA respectively). In addition to the anatomical distinction, I-CCA and E-CCA also differ with respect their growth patterns. Specifically, I-CCA tend to be mass forming and often metastasize whereas E-CCA tend to grow parallel to tissue planes and rarely develop distant metastases [1,2].

Unfortunately, CCA treatment (both l-CCA and E-CCA) is often palliative. Surgical excision and liver transplantation are potentially curative but can only be offered to a small minority of CCA patients [3–6]. Chemotherapy and radiation therapy are largely ineffective.

Thus, it is not surprising that mean overall CCA patient survival times are less than two years [7,8].

Chemokines are 8–14 kDa proteins consisting of four main subclasses: C-, CC-, CXC- and CX_3C- where C represents cysteine and X any amino acid residue. Beyond their traditional roles of modulating immune cell trafficking [9], chemokine receptors (CRs: CC, CXC, XC or CX_3C-R) and ligands (-L) also regulate non-immune cell growth and migration [9,10].

In the setting of carcinoma, chemokine gradients within the tumor microenvironment influence tumor cell survival, growth and metastasis [11]. A well-studied example is the chemotaxis complex: chemokine receptor CXCR4 and its ligand CXCL12. This receptor-ligand interaction has been implicated in the development of tumor metastases for in excess of 20 distinct tumor types [12]. In addition, CR and chemokine interactions influence tumor angiogenesis and the induction of tumor promoting growth factors [11,13,14].

Despite the high mortality associated with CCA and importance of chemotaxis in regulating tumor cell biology, there are a paucity

* Corresponding author.
E-mail address: gerald.minuk@umanitoba.ca (G.Y. Minuk).

Abbreviations

CCR	chemokine receptors
I-CCA	intra-hepatic cholangiocarcinoma
E-CCA	extra-hepatic cholangiocarcinoma
WST-1	water-soluble tetrazolium salt-1
RANTES	regulated on activation, normal T cell expressed and secreted
FBS	fetal bovine serum
mTOR	mechanistic target of rapamycin
CSC	cancer stem cells

of reports describing chemotaxis in CCA. In one of the few studies reported to date, CXCR4-CXCL12 interactions were described in both CCA tissues and cell lines [15]. In another, inhibition of CXCR4 expression reduced CCA tumor cell proliferation, metastasis and neural invasion whereas overexpression induced tumor cell invasion [16–20]. Finally, CXCR2-CXCL5 interactions have been implicated in CCA tumor development and inhibition of CXCR2 expression has been reported to significantly inhibit tumor growth [21]. To date, there have been no reports describing the expression profile or influence of the CCR subclass on I-CCA and E-CCA tumor cell biology.

In the present study, we documented the CCR subclass expression profiles (CCR1-10) in representative human I-CCA and E-CCA cell lines. We also documented the effects of a commercially available CCR5 antagonist (Maraviroc) and agonist (RANTES) on I-CCA and E-CCA proliferation, spheroid formation, migration and invasion.

2. Materials and methods

2.1. Cells and reagents

The human I-CCA HuCCT1 cell line was purchased from Sekisui XenoTech (USA), and E-CCA KMBC cell line from ATCC (USA). Maraviroc, a commercially available CCR5 antagonist was purchased from Sigma-Aldrich, USA, and RANTES, a CCR5 agonist from Invitrogen, USA.

2.2. Cell culture

HuCCT1 and KMBC cells were cultured in RPMI 1640 medium supplemented with 110 mg/L sodium pyruvate, 10% HI- fetal bovine serum (FBS), 100 U/mL penicillin and 100 μg/mL streptomycin (Invitrogen, USA). All cells were incubated at 37 °C in a humidified atmosphere of 5% CO_2 and 95% air.

2.3. CCR expression profiles

Total RNA was extracted by TRIzol Plus RNA Purification (Invitrogen, USA). First strand cDNA was synthesized by the iScript[TM] cDNA synthesis kit Reverse Transcription Kit (Bio-Rad, USA) according to the manufacturer's instructions. Real-time polymerase chain reaction (qPCR) was performed using the Power SYBR® Green PCR Master Mix (Invitrogen, USA). The specific primers are listed in Table 1 and were designed with the respective sequences from GenBank by Oligo 7 software. PCR amplification was initially held at 95 °C for 10 min, then carried out by applying 35 cycles comprised of denaturation at 95 °C for 15 s, annealing temperature at 58 °C for 1 min, followed by a final melting curve stage using a ViiA[TM] 7 Real-time PCR System (Applied Bio-systems, USA). Data were analyzed by QuantStudio[TM] Real-Time PCR Software (Applied Bio-systems, USA). The gene cycle threshold (CT) value of the target was normal-

Table 1
Primers and conditions of real-time polymerase chain reaction.

Genes	Primers (5′–3′)	Tm (°C)	Size (bp)
CCR1			
Sense	GACTATGACACGACCACAGAGT	60	117
Anti-sense	TACCAAGGAGTACAGAGGGGG		
CCR2			
Sense	AGTTCAGAAGGTATCTCTCGGTG	60	115
Anti-sense	GGCGTGTTTGTTGAAGTCACT		
CCR3			
Sense	GTCATCATGGCGGTGTTTTTC	60	155
Anti-sense	CAGTGGGAGTAGGCGATCAC		
CCR4			
Sense	AGAAGGCATCAAGGCATTTGG	60	137
Anti-sense	ACACATCAGTCATGGACCTGAG		
CCR5			
Sense	TTCTGGGCTCCCTACAACATT	60	93
Anti-sense	TTGGTCCAACCTGTTAGAGCTA		
CCR6			
Sense	TTCAGCGATGTTTTCGACTCC	60	134
Anti-sense	GCAATCGGTACAAATAGCCTGG		
CCR7			
Sense	TGAGGTCACGGACGATTACAT	60	134
Anti-sense	GTAGGCCCACGAAACAAATGAT		
CCR8			
Sense	GTGTGACAACAGTGACCGACT	60	173
Anti-sense	CTTCTTGCAGACCACAAGGAC		
CCR9			
Sense	ATGTCAGGCAGTTTGCGAG	60	105
Anti-sense	TGCAGTACCAGTAGACAAGGAT		
CCR10			
Sense	ATTACTCTGGGGATGAAGA	56	117
Anti-sense	CCACGGTCAGGGAGACACT		
β-actin			
Sense	TCCTCTCCCAAGTCCACACAGG	60	131
Anti-sense	GGGCACGAAGGCTCATCATTC		

ized to beta-actin. Gene expressions were calculated by using the relative quantification method ($2^{-\Delta CT}$) [22].

2.4. Cell proliferation

HuCCT-1 and KMBC cells were seeded onto 96-well plates at a density of 5000 cells per well in 100 μL of RPMI 1640 medium with 10% FBS and incubated for 24 h. The following day, cell culture media (CM) was replaced with 5% heat inactivated FBS (Invitrogen, USA). During concentration-dependent experiments, cells were exposed to CM alone or CM plus a range of Maravirocs (0.1–1000 nM) and RANTES (1–50 ng/mL) concentrations for three days. Time-dependent proliferative activity was tested from days 1 to 6 at CM alone or CM plus a constant Maraviroc concentration of 1000 nM, RANTES 20 ng/mL or a combination of Maraviroc/RANTES (1000 nM/20 ng/mL). At the end of treatments, cell proliferation was measured by adding premixed WST-1 reagent (Takara Bro, USA) and incubating at 37 °C for 3 h. Blank wells with CM alone were used to detect background activity.

2.5. Spheroid formation

HuCCT1 and KMBC cell lines were suspended in Dulbecco's Modified Eagle Medium/Nutrient Mixture F-12 (DMEM/F12) medium (Invitrogen, USA), supplemented with $1 \times$ B-27 Serum-Free Supplement (Invitrogen, USA), 4 μg/mL heparin (Stem cell Technologies, Canada), 100 U/mL penicillin and 100 μg/mL streptomycin, 10 ng/mL epidermal growth factor (EGF) (Invitrogen, USA), and 10 ng/mL basic fibroblast growth factor (bFGF) (Invitrogen, USA) [23]. Cells were subsequently seeded at densities of 200 cells per well in ultra-low attachment 96-well plates (Corning, USA), and treated with either Maraviroc (1000 nM), RANTES (20 ng/mL), or Maraviroc/RANTES (1000 nM/20 ng/mL). After 0, 3 and 6 days of
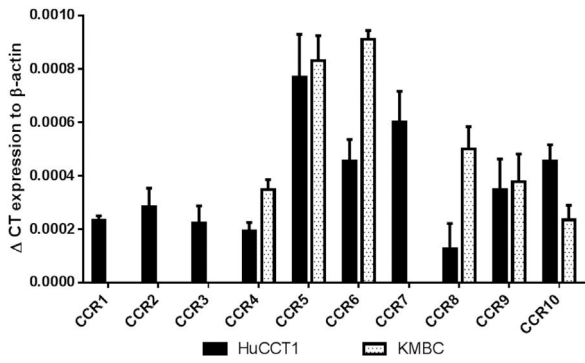
Fig. 1. CCR subtype mRNA expression in HuCCT1 and KMBC cells as determined by real-time RT-PCR. Human activated peripheral blood mononuclear cells (PBMCs) served as positive controls. Data presented as mean ± SD of three determinations.

culture, spheroids were photographed using an inverted microscope (Optika, Italy). Cells treated with CM only served as the controls. Aggregation diameter was measured and analyzed using ImageJ software.

2.6. Cell migration

HuCCT1 and KMBC cell lines (0.5×10^6/mL, 2 mL per well) were seeded in 6-well plates and cultured with RPMI 1640 medium supplemented with 10% FBS until confluent. Monolayers were then scratched with a 200 µL pipette tip to generate a wound according to the method described previously [24]. To investigate the effects of Maraviroc, RANTES and Maraviroc/RANTES on wound healing, cells were exposed to Maraviroc (1000 nM), RANTES (20 ng/mL), and Maraviroc/RANTES (1000 nM/20 ng/mL). Phase contrast images were captured at 0, 12 and 24 h. Images acquired for each cell group were analyzed quantitatively by using ImageJ software. By comparing images from each captured time point, the migration capacity of cells was measured as the extent of wound closure by calculating wound area.

2.7. Cell invasion

Twenty-four well Transwell permeable supports with 8 µm pores (Corning, USA) were used to measure cell invasion. HuCCT1 or KMBC cells (1×10^5) in 100 µL serum-free medium were added to the upper chambers. The lower chambers contained 650 µL RPMI 1640 medium with either 10% FBS, 5% heat inactivated FBS,
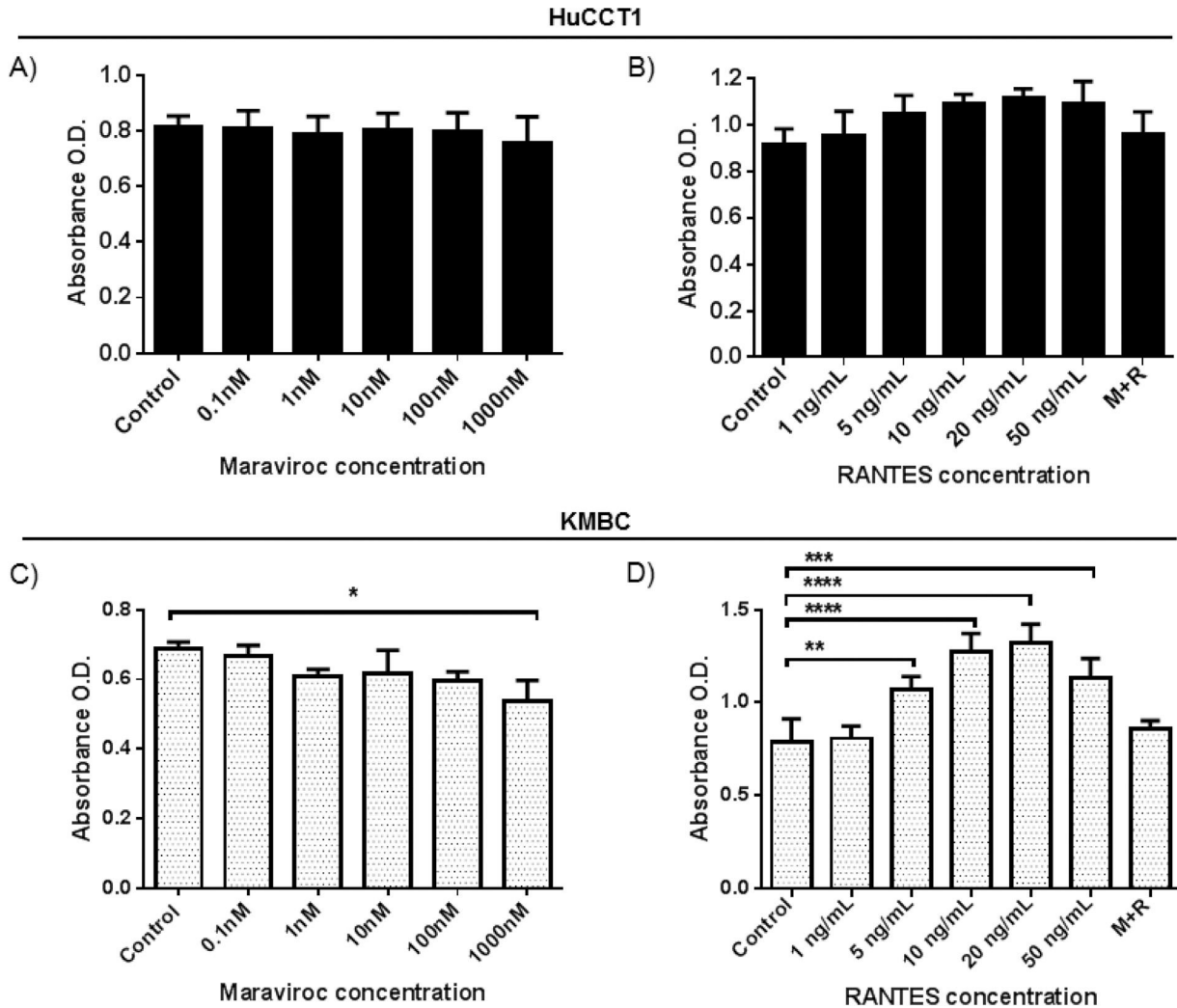

Fig. 2. Dose-dependent effects of the CCR5 antagonist (Maraviroc) and agonist (RANTES) on HuCCT1 and KMBC cell proliferation. HuCCT1 and KMBC cells were exposed to Maraviroc or RANTES for 3 days. Panels A and B: Dose-dependent effects of Maraviroc and RANTES on HuCCT1 cell and Panels C and D: KMBC cell proliferation. The stimulatory effects of RANTES on KMBC cell proliferation were no longer evident when KMBC cells were exposure to the combination of Maraviroc/RANTES (M + R). Data presented as mean ± SD. *: $p < 0.05$, **: $p < 0.01$, ***: $p < 0.001$, ****: $p < 0.0001$.
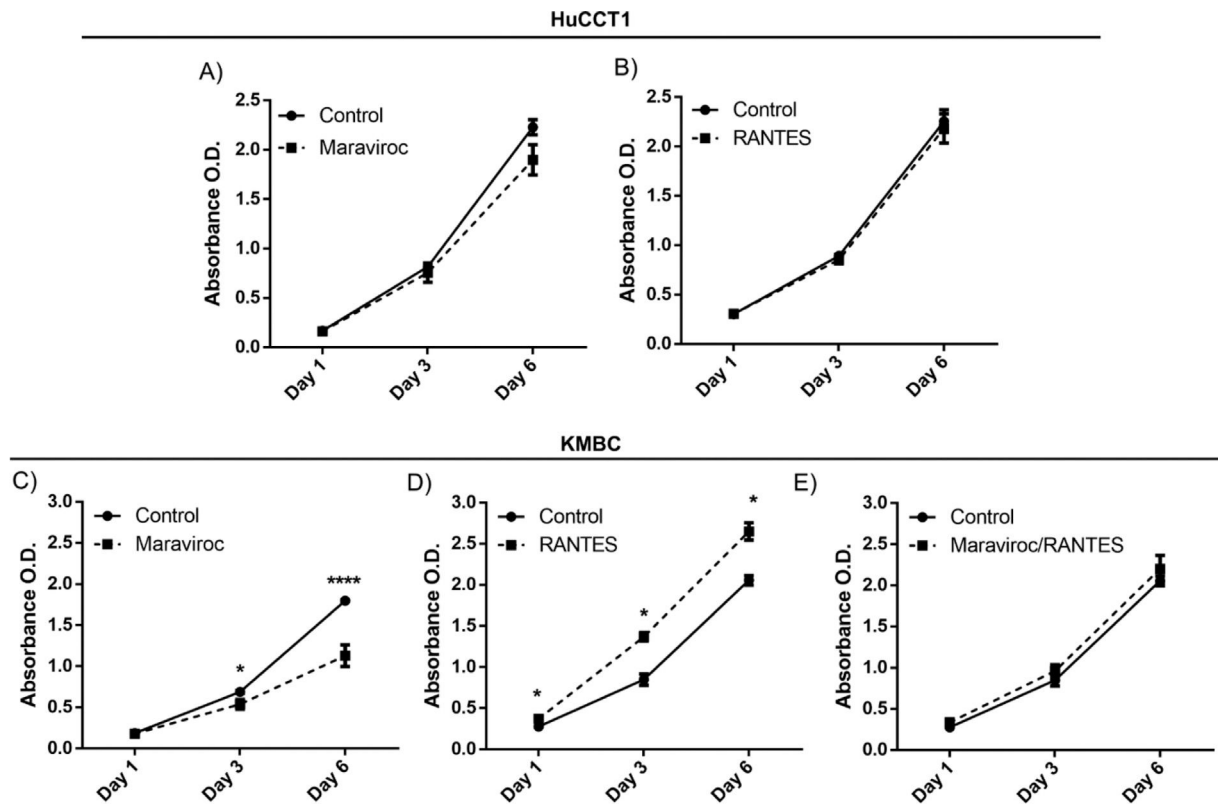
Fig. 3. Time-dependent effects of the CCR5 antagonist (Maraviroc) and agonist (RANTES) on HuCCT1 and KMBC cell proliferation. HuCCT1 and KMBC cells were exposed to Maraviroc, RANTES, or Maraviroc/RANTES for 1, 3, and 6 days. Panels A and B: Time-dependent effects of Maraviroc (1000 nM) and RANTES (20 ng/mL) on HuCCT1 cell proliferation. Panels C and D: Time-dependent effects of Maraviroc (1000 nM) and RANTES (20 ng/mL) on KMBC cells. The inhibitory effects of Maraviroc on days 3 and 6 and stimulatory effects of RANTES at all time points on KMBC cell proliferation were no longer evident when KMBC cells were exposure to the combination of Maraviroc/RANTES (Panel E). Data presented as mean ± SD. *: $p < 0.05$.

Maraviroc (1000 nM), RANTES (20 ng/mL), or Maraviroc/RANTES (1000 nM/20 ng/mL). After 24 h incubation, cells from the upper surface membrane were removed with a cotton swab. Penetrated cells in the lower chamber were dissociated and collected by a cell dissociation buffer (Invitrogen, USA). Collected cells were counted by a cell counter (Cellometer® Auto 2000, Nexcelom Bioscience, USA).

2.8. Statistical analysis

All experiments were performed in triplicate and repeated on a minimum of three occasions. Significant differences were determined by repeated measures of ANOVA and/or Tukey's multiple comparison post hoc test. A Student's *t*-test was used for comparisons of two groups. Data were analyzed by GraphPad Prism 6 statistical software (GraphPad Software, Inc., USA). Differences with p values below 0.05 were considered statistically significant.

3. Results

The CCR expression profiles of HuCCT1 and KMBC cells are provided in Fig. 1. All 10 CCR motifs (CCR1-10) were expressed in HuCCT1 cells, while six (CCR4, CCR5, CCR6, CCR8, CCR9 and CCR10) were detected in KMBC cells. The CCR motifs most abundant in HuCCT1 cells were CCR5 followed by CCR7. In KMBC cells, CCR6 was most abundant followed by CCR5. Thus, as one of the higher CCR expressed subtypes, the effects of the CCR5 antagonist Maraviroc, agonist RANTES and Maraviroc/RANTES combination on I-CCA and E-CCA cell biology were further explored.

As shown in Fig. 2A and B, in HuCCT1 cells, there were no concentration-dependent alterations in cell proliferation with Maraviroc or RANTES. However, in KMBC cells (Fig. 2C and D), proliferation was inhibited at the highest concentration of Maraviroc (1000 nM), and upregulated at RANTES concentrations of 5 ng/mL and higher with maximum increased proliferation occurring at 20 ng/mL. Based on these findings, all further experimentation was performed at a Maraviroc concentration of 1000 nM, RANTES 20 ng/mL and Maraviroc/RANTES (1000 nM/20 ng/mL). Of note, the increase in KMBC cell proliferation that occurred with RANTES was not observed following exposure to the combination of Maraviroc/RANTES (data not shown).

There were no time-dependent effects of Maraviroc or RANES on HuCCT1 cell proliferation over the six days exposure (Fig. 3A). However, in KMBC cells, an inhibitory effect of Maraviroc on cell proliferation was evident on day 3 and more so on day 6 ($p < 0.05$ and 0.0001 respectively) (Fig. 3C). On exposure to RANTES, KMBC cell proliferation increased at all time periods (Fig. 3D). In the presence of both Maraviroc/RANTES, the inhibitory effects of Maraviroc and stimulatory effects of RANTES were no longer evident (Fig. 3E).

Fig. 4 demonstrates the results of spheroid formation in HuCCT1 and KMBC cells following treatment with Maraviroc, RANTES, or Maraviroc/RANTES. Neither Maraviroc, RANTES nor Maraviroc/RANTES altered spheroid information in HuCCT1 cells (Fig. 4A). On the other hand, spheroid formation was significantly inhibited in KMBC cells following exposure to Maraviroc (Day 3 dimensions for Maraviroc: 145 ± 6 nM versus control: 244.7 ± 11.2 nM, $p < 0.0001$; Day 6: Maraviroc: 170.7 ± 17.6 nM versus control: 322.7 ± 23.7 nM, $p < 0.0001$), while RANTES alone had no effect. In the presence of both Maraviroc/RANTES, the inhibitory effect of Maraviroc on KMBC cells was no longer evident.
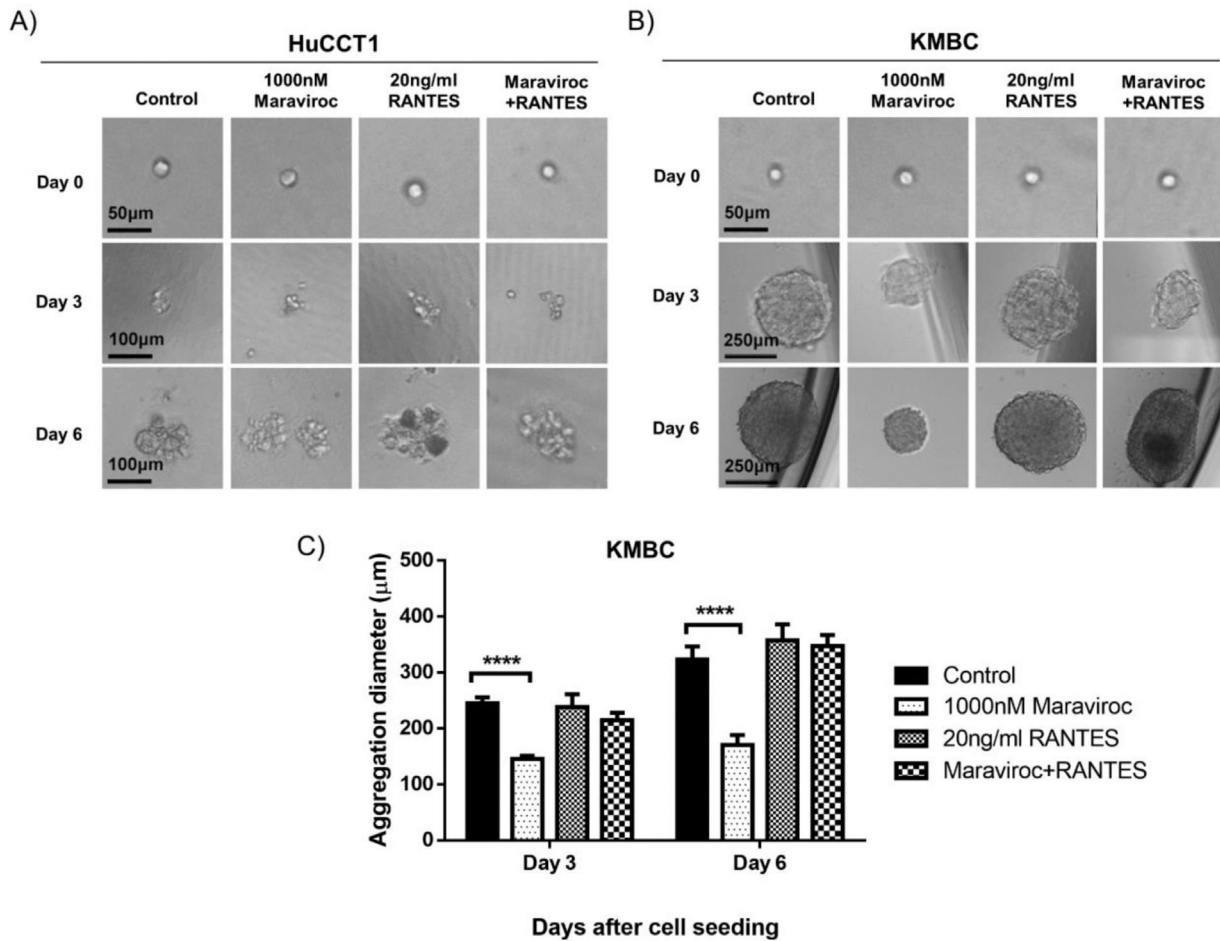
Fig. 4. Spheroid formation by HuCCT1 and KMBC cells in the presence of the CCR5 antagonist Maraviroc (1000 nM), agonist RANTES (20 ng/mL), and a combination of Maraviroc/RANTES (1000 nM/20 ng/mL). Cells were seeded at densities of 200 cells/well in ultra-low 96-well plates to generate spheroids. Panel A: Spheroid formation in HuCCT1 cells was not influenced by Maraviroc, RANTES, or Maraviroc/RANTES. Sale bar: 50 and 100 μm. Panel B: Maraviroc inhibited KMBC spheroid formation on days 3 and 6 while RANTES had no effect. The inhibitory effect of Maraviroc was no longer evident when KMBC cells were exposed to the combination of Maraviroc/RANTES. Sale bar: 50 and 250 μm. Panel C: The diameters of spheroid formation were measured by software ImageJ. Data presented as mean ± SD. ****: $p < 0.0001$.

The effects of Maraviroc, RANTES and Maraviroc/RANTES on cell migration were documented by the scratch wound healing assay (Fig. 5). Here, Maraviroc inhibited HuCCT1 cell migration at 12 h (Fig. 5A and B), while RANTES had no significant effect. The inhibitory effect of Maraviroc was no longer evident in the presence of Maraviroc/RANTES. In KMBC cells the inhibition of Maraviroc at 12 and 24 h was not significant but increases in cell migration occurred with RANTES at both time intervals. In the presence of Maraviroc/RANTES, the increases associated with RANTES alone were no longer evident (Fig. 5C and D).

Finally, regarding cell invasion, Maraviroc inhibited HuCCT1 cell invasion (Fig. 6A), whereas RANTES had no effect. The inhibitory effect of Maraviroc was no longer evident in the presence of Maraviroc/RANTES. In KMBC cells, Maraviroc inhibited while RANTES increased cell invasion (Fig. 6B). Of note, the increase observed with RANTES persisted in the presence of Maraviroc/RANTES.

4. Discussion

The results of this study indicate that CCR expression profiles differed in these representative human I-CCA and E-CCA cell lines. The results also indicate that a specific CCR5 antagonist and agonist, can alter tumor cell biology in a cell-specific manner with the CCR5 antagonist being associated with attenuated and agonist, enhanced tumor cell activities. Together, these findings could help to explain the different tumor growth characteristics observed in I-CCA and E-CCA. They also raise the possibility that CCR5 antagonists may have therapeutic benefit in the treatment of CCA.

Unfortunately there have been no previous reports documenting the complete CCR expression profile in human CCA tissues or cell lines. Thus, a comparative analysis with previous data could not be undertaken. However, the CCR expression profile detected in I-CCA was similar to that described for human hepatocellular carcinoma [25], a finding that may reflect the common risk factors and/or origin of these tumors [26]. Moreover, significant expression of CCR5 is in keeping with the high expression observed in the livers of patients with chronic liver disease and its tumor promoting properties which include activation of mTOR and AKT pathways [27].

Overall, the CCR5 antagonist Maraviroc inhibited HuCCT1 growth promoting properties and to a lesser extent, in KMBC cells. Specifically, Maraviroc inhibited HuCCT1 proliferation, migration and invasion whereas in KMBC cells, spheroid formation and invasion were inhibited. Somewhat surprisingly, with the exception of KMBC cell invasion, RANTES alone did not have opposing effects. Presumably, this finding relates to constitutive CCR5 activation by an autocrine ligand [28]. That the addition of Maraviroc did not reverse the increase in cell invasion associated with RANTES, suggests the RANTES effect may be CCR5-independent. However, it is also possible the process is concentration-dependent and
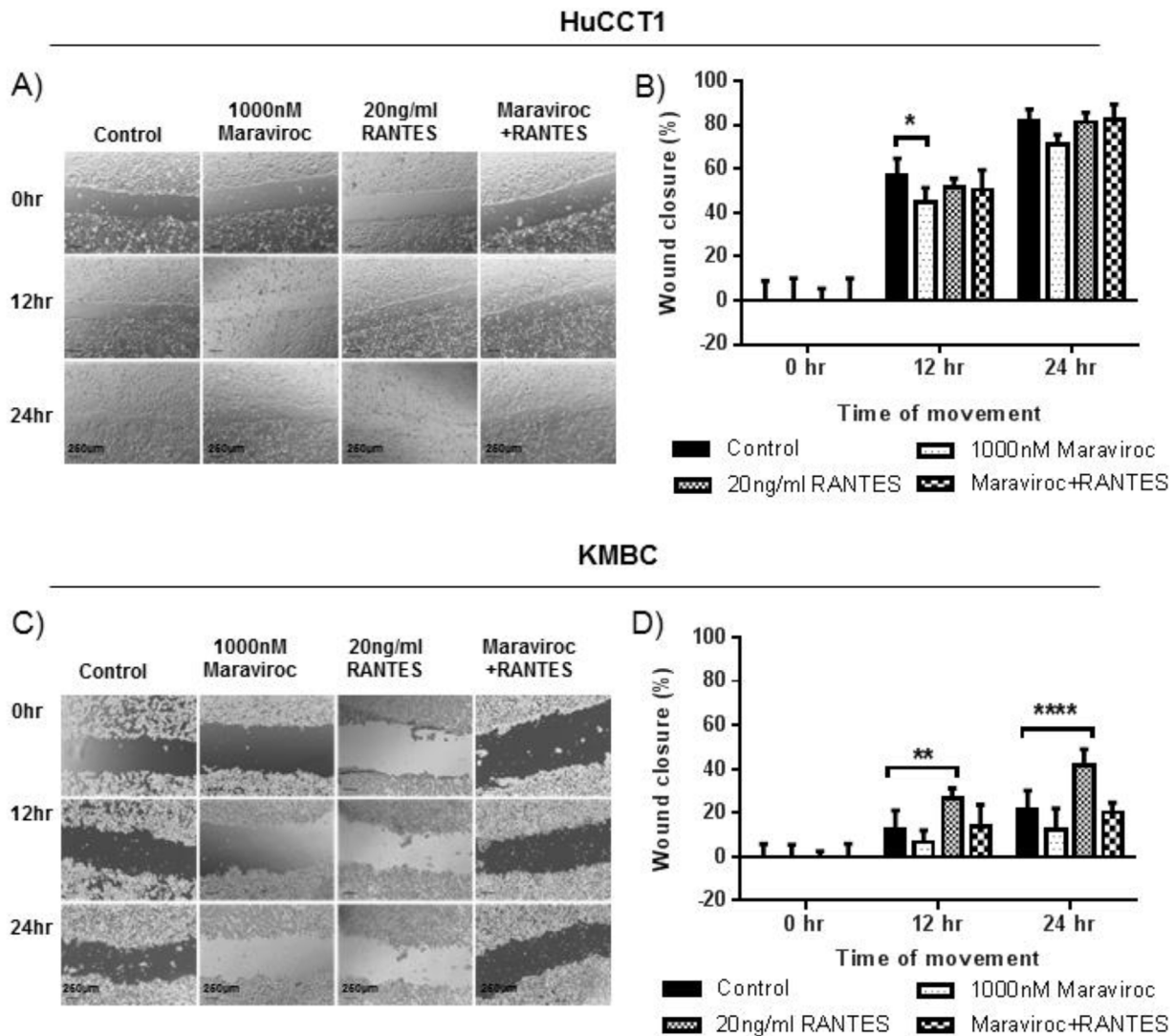
Fig. 5. Migration of HuCCT1 and KMBC cells after exposure to the CCR5 antagonist Maraviroc (1000 nM), agonist RANTES (20 ng/mL) and combination of Maraviroc/RANTES (1000 nM/20 ng/mL). Panels A and B: Results in HuCCT1cells, and Panels C and D: in KMBC cells. Maraviroc delayed HuCCT1 wound closure at 12 h while RANTES increased KMBC wound closure at 12 and 24 h. Both the inhibitory effects of Maraviroc and stimulatory effects of RANTES were no longer evident when cells were exposed to the combination of Maraviroc/RANTES. Sale bar: 250 μm. ImageJ analysis of cell migration was determined by measuring wound closure from phase-contrast images. Data presented as mean ± SD. *: $p < 0.05$; **: $p < 0.01$; ****: $p < 0.0001$.

higher concentrations of Maraviroc may have been more effective.

In terms of clinical relevance, the results of this study and those obtained with the commercially available CCR5 antagonist Maraviroc in particular, suggest that in CCA, therapeutic benefit might be derived from CCR5 inhibition. Such an approach has been applied to gastric cancers with some success [29]. The possibility is rendered feasible by the fact the inhibitory concentration of Maraviroc (1000 nM) is well within the range reported in the blood of patients treated with this agent [30]. Also to be considered is whether the use of a CCR5 antagonist in the treatment of primary sclerosing cholangitis (PSC), a condition associated with a significantly increased risk of CCA, may help to prevent the development or course of these tumors in PSC patients.

Having confirmed that at least in these two cell lines, I-CCA and E-CCA possess different CCR expression profiles and respond differently to a CCR5 antagonist and agonist, the question arises as to why such differences exist. Both I-CCA and E-CCA consist of malignant cholangiocytes. However, when analyzed for differences in the expression of cancer stem cell (CSC) markers, significant differences are evident. Specifically, CSC markers are expressed in greater than 90% of HuCCT1 cells but less than 5% of KMBCs cells (authors unpublished data). Given that the prevalence of CSCs influences tumor cell biology, this could explain the differences observed. Clearly, further research is required to test this hypothesis.

There are a number of limitations to this study that warrant emphases. First, only one I-CCA and one E-CCA cell line were studied. Whether similar results would have been obtained with additional cell lines remains to be determined. Second, due to the lack of commercially available CCR antagonists other than Maraviroc, only the effects of CCR5 inhibition were documented. When available, results obtained with a CCR6 antagonist, the CCR subtype expressed to the greatest extent in KMBC cells, will be of interest. Third, because CCR5 receptor inhibition and activation with Maraviroc and RANTES respectively have been documented in all other cells studied to date, confirmation of the effects of these agents on receptor activity per se was not undertaken. Finally, the results
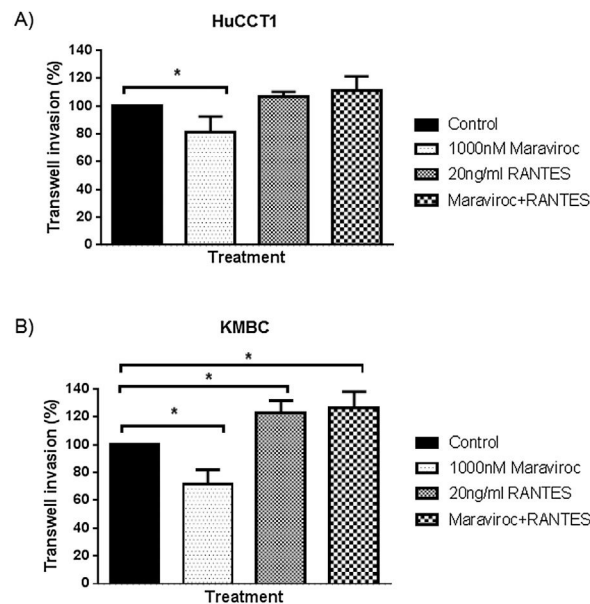
Fig. 6. Invasion of HuCCT1 and KMBC cells were documented with the use of Transwell invasion chambers, in the presence of Maraviroc (1000 nM), RANTES (20 ng/mL) and the combination of Maraviroc/RANTES combination (1000 nM/20 ng/mL). Panel A: Results in HuCCT1 cells and Panel B: in KMBC cells. Maraviroc inhibited HuCCT1 and KMBC cell invasion while RANTES increased KMBC cell invasion. The stimulatory effect of RANTES on KMBC cell persisted in the presence of Maraviroc/RANTES. Data presented as mean ± SD. *: $p < 0.05$.

described reflect preliminary findings of an in vitro cell based system. Additional studies in animal models of CCA are warranted.

In conclusion, the results of this study support clinical observations that I-CCA and E-CCA have different tumor growth and invasive properties. They also raise the possibility that these differences reflect differences in CCR expression profiles. In general, exposure to a specific CCR5 antagonist inhibited while an agonist enhanced tumor cell properties. Additional studies are required to determine whether inhibition of CCR5 has benefit in the treatment of CCA in humans.

Lay summary

Activation of chemokine receptors can alter the behavior of normal and cancerous cells. This study revealed that bile duct cancers which develop within the liver express different chemokine receptors than those that develop outside the liver. This finding may help to explain why the two types of bile duct cancer behave differently. Importantly, the results also indicate the behavior of bile duct cancer cells can be favorably altered by blocking certain chemokine receptors.

Financial support

Contributions

Concept & design: JY, YG, GYM. Experiments and procedures: JY, DS. Data analysis: JY, YG, GYM. Writing of article: JY, YG, GYM.

Conflict of interest

There are no conflicts of interest to report.

References

[1] Nakeeb A, Pitt HA, Sohn TA, Coleman J, Abrams RA, Piantadosi S, et al. Cholangiocarcinoma. A spectrum of intrahepatic, perihilar, and distal tumors. Ann Surg 1996;224(4):463–73, discussion 73-5.

[2] Zhang XF, Bagante F, Chen Q, Beal EW, Lv Y, Weiss M, et al. Perioperative and long-term outcome of intrahepatic cholangiocarcinoma involving the hepatic hilus after curative-intent resection: comparison with peripheral intrahepatic cholangiocarcinoma and hilar cholangiocarcinoma. Surgery 2018;163(5):1114–20.

[3] DeOliveira ML, Cunningham SC, Cameron JL, Kamangar F, Winter JM, Lillemoe KD, et al. Cholangiocarcinoma: thirty-one-year experience with 564 patients at a single institution. Ann Surg 2007;245(5):755–62.

[4] Nagino M, Kamiya J, Nishio H, Ebata T, Arai T, Nimura Y. Two hundred forty consecutive portal vein embolizations before extended hepatectomy for biliary cancer: surgical outcome and long-term follow-up. Ann Surg 2006;243(3):364–72.

[5] Mavros MN, Economopoulos KP, Alexiou VG, Pawlik TM. Treatment and prognosis for patients with intrahepatic cholangiocarcinoma: systematic review and meta-analysis. JAMA Surg 2014;149(6):565–74.

[6] Petrowsky H, Hong JC. Current surgical management of hilar and intrahepatic cholangiocarcinoma: the role of resection and orthotopic liver transplantation. Transpl Proc 2009;41(10):4023–35.

[7] Cho SY, Park SJ, Kim SH, Han SS, Kim YK, Lee KW, et al. Survival analysis of intrahepatic cholangiocarcinoma after resection. Ann Surg Oncol 2010;17(7):1823–30.

[8] Lee SJ, Kwon W, Kang MJ, Jang JY, Chang YR, Jung W, et al. Clinical features and survival outcome of locally advanced extrahepatic cholangiocarcinoma. Korean J Hepato-biliary-pancreatic Surg 2014;18(1):1–8.

[9] Charo IF, Ransohoff RM. The many roles of chemokines and chemokine receptors in inflammation. N Engl J Med 2006;354(6):610–21.

[10] Miyazaki H, Takabe K, Yeudall WA. Chemokines, chemokine receptors and the gastrointestinal system. World J Gastroenterol 2013;19(19):2847–63.

[11] Balkwill F. Cancer and the chemokine network. Nat Rev Cancer 2004;4(7):540–50.

[12] Balkwill F. The significance of cancer cell expression of the chemokine receptor CXCR4. Semin Cancer Biol 2004;14(3):171–9.

[13] Chow MT, Luster AD. Chemokines in cancer. Cancer Immunol Res 2014;2(12):1125–31.

[14] Zheng K, Li HY, Su XL, Wang XY, Tian T, Li F, et al. Chemokine receptor CXCR7 regulates the invasion, angiogenesis and tumor growth of human hepatocellular carcinoma cells. J Exp Clin Cancer Res 2010;29:31.

[15] Leelawat K, Leelawat S, Narong S, Hongeng S. Roles of the MEK1/2 and AKT pathways in CXCL12/CXCR4 induced cholangiocarcinoma cell invasion. World J Gastroenterol 2007;13(10):1561–8.

[16] Ohira S, Sasaki M, Harada K, Sato Y, Zen Y, Isse K, et al. Possible regulation of migration of intrahepatic cholangiocarcinoma cells by interaction of CXCR4 expressed in carcinoma cells with tumor necrosis factor-alpha and stromal-derived factor-1 released in stroma. Am J Pathol 2006;168(4):1155–68.

[17] Tan XY, Chang S, Liu W, Tang HH. Silencing of CXCR4 inhibits tumor cell proliferation and neural invasion in human hilar cholangiocarcinoma. Gut Liver 2014;8(2):196–204.

[18] Xie Y, Wehrkamp CJ, Li J, Wang Y, Wang Y, Mott JL, et al. Delivery of miR-200c mimic with poly(amido amine) cxcr4 antagonists for combined inhibition of cholangiocarcinoma cell invasiveness. Mol Pharmaceut 2016;13(3):1073–80.

[19] Zhao S, Wang J, Qin C. Blockade of CXCL12/CXCR4 signaling inhibits intrahepatic cholangiocarcinoma progression and metastasis via inactivation of canonical Wnt pathway. J Exp Clin Cancer Res 2014;33:103.

[20] Leelawat K, Keeratichamroen S, Leelawat S, Tohtong R. CD24 induces the invasion of cholangiocarcinoma cells by upregulating CXCR4 and increasing the phosphorylation of ERK1/2. Oncol Lett 2013;6(5):1439–46.

[21] Sueoka H, Hirano T, Uda Y, Iimuro Y, Yamanaka J, Fujimoto J. Blockage of CXCR2 suppresses tumor growth of intrahepatic cholangiocellular carcinoma. Surgery 2014;155(4):640–9.

[22] Livak KJ, Schmittgen TD. Analysis of relative gene expression data using real-time quantitative PCR and the 2(-Delta Delta C(T)) Method. Methods 2001;25(4):402–8.

[23] Yang J, Gong Y, Sontag DP, Corbin I, Minuk GY. Effects of low-density lipoprotein docosahexaenoic acid nanoparticles on cancer stem cells isolated from human hepatoma cell lines. Mol Biol Rep 2018;45(5):1023–36.

[24] Liang CC, Park AY, Guan JL. In vitro scratch assay: a convenient and inexpensive method for analysis of cell migration in vitro. Nat Protoc 2007;2(2):329–33.

[25] Liang CM, Chen L, Hu H, Ma HY, Gao LL, Qin J, et al. Chemokines and their receptors play important roles in the development of hepatocellular carcinoma. World J Hepatol 2015;7(10):1390–402.

[26] Feng DF, Gong P, Li W, Xu H, Zhang T, Wang N. Identification and characterization of tumorigenic liver cancer stem cells by CD133 and CD24. J Biomater Tissue Eng 2015;5:635–46.

[27] Weitzenfeld P, Ben-Baruch A. The chemokine system, and its CCR5 and CXCR4 receptors, as potential targets for personalized therapy in cancer. Cancer Lett 2014;352(1):36–53.

[28] Long H, Xie R, Xiang T, Zhao Z, Lin S, Liang Z, et al. Autocrine CCL5 signaling promotes invasion and migration of CD133+ ovarian cancer stem-like cells via NF-kappaB-mediated MMP-9 upregulation. Stem Cells 2012;30(10):2309–19.

[29] Mencarelli A, Graziosi L, Renga B, Cipriani S, D'Amore C, Francisci D, et al. CCR5 antagonism by maraviroc reduces the potential for gastric cancer cell dissemination. Transl Oncol 2013;6(6):784–93.

[30] Rosario MC, Jacqmin P, Dorr P, James I, Jenkins TM, Abel S, et al. Population pharmacokinetic/pharmacodynamic analysis of CCR5 receptor occupancy by maraviroc in healthy subjects and HIV-positive patients. Br J Clin Pharmacol 2008;65(Suppl. 1):86–94.